EuroIntervention
2024;20:e669-e680
published online e-edition May 2024
DOI: 10.4244/EIJ-D-23-00563

ORIGINAL RESEARCH

Ultrathin-strut versus thin-strut stent healing and outcomes in preclinical and clinical subjects

Ryutaro Ikegami[1,2], MD, PhD; Zhonglie Piao[3], PhD; Juan F. Iglesias[4], MD, PhD; Thomas Pilgrim[5], MD; Khanh Ha[6,7], PhD; Jason R. McCarthy[6,7], PhD; Maria I. Castellanos[8,9], PhD; Mohamad B. Kassab[1], MD; Mazen S. Albagdadi[1,10], MD, MSc; Adam Mauskapf[1], BS; Graham Spicer[3], PhD; David E. Kandzari[11], MD; Elazer R. Edelman[12,13,14], MD, PhD; Peter Libby[14], MD; Dik Heg[15], PhD; Michael Joner[8,9], MD; Guillermo J. Tearney[3,12], MD, PhD; Farouc A. Jaffer[1,3]*, MD, PhD

R. Ikegami and Z. Piao contributed equally to this manuscript.
G.J. Tearney and F.A. Jaffer shared senior authorship.

**Corresponding author: Cardiovascular Research Center, Division of Cardiology, Massachusetts General Hospital, Boston, MA, USA. E-mail: fjaffer@mgh.harvard.edu*

The authors' affiliations can be found at the end of this article.

This paper also includes supplementary data published online at: https://eurointervention.pcronline.com/doi/10.4244/EIJ-D-23-00563

ABSTRACT

BACKGROUND: Compared with thin-strut durable-polymer drug-eluting stents (DP-DES), ultrathin-strut biodegradable-polymer sirolimus-eluting stents (BP-SES) improve stent-related clinical outcomes in patients undergoing percutaneous coronary intervention (PCI). Reduced stent strut thickness is hypothesised to underlie these benefits, but this conjecture remains unproven.

AIMS: We aimed to assess the impact of strut thickness on stent healing and clinical outcomes between ultrathin-strut and thin-strut BP-SES.

METHODS: First, we performed a preclinical study of 8 rabbits implanted with non-overlapping thin-strut (diameter/thickness 3.5 mm/80 µm) and ultrathin-strut (diameter/thickness 3.0 mm/60 µm) BP-SES in the infrarenal aorta. On day 7, the rabbits underwent intravascular near-infrared fluorescence optical coherence tomography (NIRF-OCT) molecular-structural imaging of fibrin deposition and stent tissue coverage, followed by histopathological analysis. Second, we conducted an individual data pooled analysis of patients enrolled in the BIOSCIENCE and BIOSTEMI randomised PCI trials treated with ultrathin-strut (n=282) or thin-strut (n=222) BP-SES. The primary endpoint was target lesion failure (TLF) at 1-year follow-up, with a landmark analysis at 30 days.

RESULTS: NIRF-OCT image analyses revealed that ultrathin-strut and thin-strut BP-SES exhibited similar stent fibrin deposition (p=0.49) and percentage of uncovered stent struts (p=0.63). Histopathological assessments corroborated these findings. In 504 pooled randomised trial patients, TLF rates were similar for those treated with ultrathin-strut or thin-strut BP-SES at 30-day (2.5% vs 1.8%; p=0.62) and 1-year follow-up (4.3% vs 4.7%; p=0.88).

CONCLUSIONS: Ultrathin-strut and thin-strut BP-SES demonstrate similar early arterial healing profiles and 30-day and 1-year clinical outcomes.

KEYWORDS: clinical trials; drug-eluting stent; optical coherence tomography; other imaging modalities

SUBMITTED ON 13/07/2023 - REVISION RECEIVED ON 1st 10/10/2023 / 2nd 12/12/2023 / 3rd 15/01/2023 - ACCEPTED ON 16/01/2023

Compared with bare metal stents (BMS), drug-eluting stents (DES) improve clinical outcomes in patients undergoing percutaneous coronary intervention (PCI)[1]. Moreover, newer-generation DES offer improved stent designs, including reduced metallic stent platform strut thickness, and are associated with lower stent thrombosis and target lesion revascularisation (TLR) rates[2]. In particular, stent strut thickness has been a focus of newer stent designs, as stents with thinner struts have historically outperformed stents with thicker struts from the BMS and first-generation DES eras[3,4].

After years of similar clinical outcomes among second-generation DES, newer-generation biodegradable-polymer sirolimus-eluting stents (BP-SES) containing an ultrathin-strut stent platform for certain stent sizes have demonstrated superior clinical outcomes compared to contemporary DES[5-9]. These results were driven by the BIOFLOW-V and BIOSTEMI randomised controlled trials (RCTs), which compared BP-SES (Orsiro [Biotronik]; ultrathin-strut thickness of 60 µm for 3.0 mm diameter stent, or thin-strut thickness of 80 µm for 3.5 mm diameter stent) to durable-polymer everolimus-eluting stents (DP-EES; XIENCE [Abbott]; thin-strut thickness of 81 µm for all stent diameters). However, the specific impact of ultrathin stent strut thickness remains unclear, as a hypothesis-generating subgroup analysis did not show superior outcomes for the ultrathin-strut stent subgroup[7].

In the BIOSTEMI trial, the clinical benefits of BP-SES over DP-EES emerged within 30 days[5], suggesting the potential for BP-SES to exhibit improved stent healing early on after implantation, possibly related to the ultrathin-strut thickness, proving a possible mechanism of clinical benefit. Yet mechanisms underlying the favourable outcomes with ultrathin-strut DES remain unclear, because additional factors beyond strut thickness – including stent design, stent polymer, and different sirolimus analogues – might be operative.

In this experimental and clinical study, we investigated the specific role of stent strut thickness on *in vivo* stent healing in rabbits as well as its role on clinical outcomes in BP-SES patients undergoing PCI. To specifically investigate the role of stent strut thickness without changing the underlying polymer, stent design, or sirolimus analogue, we assessed stent healing in a single stent platform with non-overlapping implanted BP-SES of 3.0 mm diameter (Orsiro; 60 µm strut thickness, ultrathin-strut) and 3.5 mm diameter (Orsiro; 80 µm strut thickness, thin-strut). To assess stent healing *in vivo* we utilised intravascular near-infrared fluorescence (NIRF) optical coherence tomography (OCT) molecular-structural fibrin imaging[10] and histopathological analysis. Next, to assess the clinical impact of ultrathin-strut versus thin-strut BP-SES, we performed a patient-level pooled analysis of PCI patients in the BIOSCIENCE and BIOSTEMI RCTs[5,11]. After stratifying patients by stent diameter (either 3.0 mm ultrathin-strut or 3.5 mm thin-strut BP-SES), we assessed target lesion failure (TLF) rates at 30 days and 1 year.

Editorial, see page e625

Impact on daily practice

This preclinical and clinical investigation of biodegradable-polymer sirolimus-eluting stents (BP-SES) demonstrates that ultrathin-strut thickness does not appear to modulate the observed benefits of BP-SES. Therefore, use of BP-SES might improve percutaneous coronary intervention outcomes independent of stent strut thickness.

Methods

IN VIVO RABBIT STUDY OF ULTRATHIN-STRUT VERSUS THIN-STRUT BP-SES STENT HEALING

The Institutional Animal Care and Use Committee at Massachusetts General Hospital approved all animal studies (2013N000015). The study design is illustrated in **Figure 1**. After balloon injury, a BP-SES 3.5 mm (80 µm, Orsiro) and a BP-SES 3.0 mm (60 µm, Orsiro) were deployed with sufficient pressure to achieve apposition in the abdominal aorta of the New Zealand white rabbits (n=8). On day 7, to assess *in vivo* fibrin-specific deposition on stent struts, the rabbits underwent NIRF-OCT imaging with the fibrin-targeted NIRF molecular imaging agent FTP11-CyAm7[10]. The rabbits were sacrificed, and the stented vessels were carefully resected, followed by *ex vivo* imaging and histological analysis. Full details are described in **Supplementary Appendix 1**.

POOLED ANALYSIS OF INDIVIDUAL PATIENT DATA FROM THE BIOSCIENCE AND BIOSTEMI TRIALS

We performed an individual patient data pooled analysis from PCI patients enrolled in the BIOSCIENCE[11] (ClinicalTrials.gov: NCT01443104; 2,119 patients: 1,063 BP-SES and 1,056 DP-EES) and BIOSTEMI[5] (ClinicalTrials.gov: NCT02579031; 1,300 patients: 649 BP-SES and 651 DP-EES) RCTs, which compared 1-year clinical outcomes after BP-SES versus DP-EES implantation with respect to the primary endpoint of TLF at 1-year follow-up, stratified by 3.0 mm or 3.5 mm stent diameter, and included a landmark analysis at 30 days. To account for differences in baseline clinical presentation between patients included in BIOSCIENCE and those included in BIOSTEMI that might influence clinical outcomes, we performed a stratification reporting clinical outcomes from each individual (BIOSCIENCE and BIOSTEMI) randomised trial **(Supplementary Appendix 1)**.

Results

EXPERIMENTAL SUBACUTE STENT HEALING IN THIN-STRUT VERSUS ULTRATHIN-STRUT BP-SES

As stent strut thickness modulates stent healing[3,4], we assessed stent healing between ultrathin-strut and thin-strut BP-SES stents in rabbits at day 7, which corresponds approximately to the clinical timepoint of 1 month in humans[12]. We compared *in vivo* healing of BP-SES with diameters of 3.5 mm and 3.0 mm implanted concomitantly in 8 rabbits by using

Abbreviations

BP-SES	biodegradable-polymer sirolimus-eluting stents	**DP-EES**	durable-polymer everolimus-eluting stents	**OCT**	optical coherence tomography
DES	drug-eluting stents	**NIRF**	near-infrared fluorescence	**PCI**	percutaneous coronary intervention
				TLF	target lesion failure

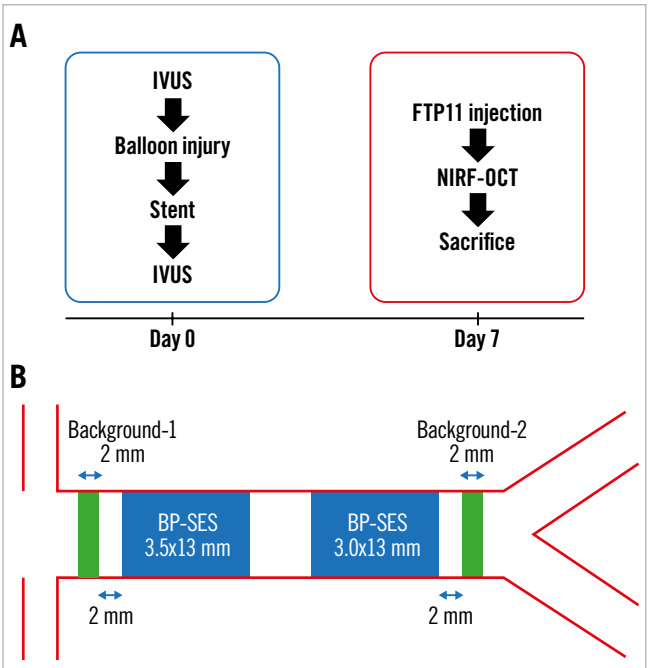

Figure 1. *Preclinical study design comparing subacute stent-healing features of ultrathin-strut and thin-strut BP-SES. A) Eight rabbits underwent implantation of non-overlapping thin-strut 3.5x13 mm and ultrathin-strut 3.0x13 mm BP-SES in the rabbit aorta and postdilated with a 3.5 mm non-compliant balloon to obtain a stent expansion ratio of 1.1-1.2 under IVUS guidance. On day 7, intravascular in vivo NIRF-OCT assessed stent healing 2 hours after intravenous FTP11-CyAm7 fibrin molecular imaging agent injection. B) The NIRF target-to-background ratio (TBR) was calculated for each stent, with the background signal averaged between at the stent proximal and distal zones 2 mm away from the stents, as indicated in green. BP-SES: biodegradable-polymer sirolimus-eluting stent; IVUS: intravascular ultrasound; NIRF: near-infrared; OCT: optical coherence tomography*

NIRF-OCT molecular imaging of fibrin and microstructural imaging of tissue coverage of the stent struts **(Figure 1B)**.

On the day of stent implantation, intravascular ultrasound (IVUS) images demonstrated a higher stent area in the 3.5 mm BP-SES group but similar stent expansion ratios for both stent sizes (p=0.91) **(Table 1)**. On day 7, *in vivo* NIRF-OCT demonstrated that the NIRF fibrin signal trended higher at the stent edge compared to the middle stent segment, for both BP-SES stent groups **(Figure 2A, Figure 2B)**. When comparing the day 7 NIRF fibrin signal target-to-background ratio (TBR) between ultrathin-strut and thin-strut BP-SES, the fibrin deposition signal did not differ significantly (32 images per stent analysed; p=0.50) **(Figure 2C)**. Likewise, the average of NIRF fibrin intensity per stent was also similar between the ultrathin-strut and thin-strut BP-SES groups (p=0.49) **(Figure 2D)**.

Ex vivo fluorescence microscopy of longitudinally opened stents confirmed that stent struts exhibiting NIRF fibrin deposition corresponded to fibrin-positive regions on *in vivo* NIRF-OCT images **(Supplementary Figure 1)**. The overall findings revealed similar *in vivo* fibrin deposition on ultrathin-strut and thin-strut BP-SES at 7 days.

Table 1. IVUS and NIRF-OCT intravascular imaging measures of stent expansion, fibrin, and coverage in BP-SES in rabbits.

	BP-SES 3.0 mm (n=8)	BP-SES 3.5 mm (n=8)	*p*-value
D0 average stent diameter, mm	3.31±0.09	3.60±0.08	<0.001
D0 average stent area, mm^2	8.77±0.42	10.37±0.47	<0.001
D0 average stent expansion ratio	1.11±0.03	1.12±0.03	0.91
D7 average stent diameter, mm	3.42±0.11	3.68±0.13	<0.01
D7 average stent area, mm^2	9.76±0.68	11.40±1.01	<0.01
D7 average stent expansion ratio	1.15±0.03	1.14±0.03	0.50
D7 average OCT-covered struts, %	2.60±0.94	2.53±0.85	0.88
D7 average OCT-uncovered struts, %	97.3±0.87	97.5±0.80	0.63
D7 average NIRF fibrin, nm	0.61±0.21	0.52±0.18	0.43
D7 average NIRF fibrin TBR	1.57±0.80	1.31±0.58	0.49

Data are presented as mean±SD. BP-SES: biodegradable-polymer sirolimus-eluting stents; D0: day 0; D7: day 7; IVUS: intravascular ultrasound; NIRF: near-infrared fluorescence; OCT: optical coherence tomography; SD: standard deviation; TBR: target-to-background ratio

Tissue coverage of stents was assessed using OCT, as previously performed[10]. On a per-strut analysis (n=260±26 struts/stent), OCT demonstrated a similarly low percentage of covered struts for both ultrathin-strut and thin-strut BP-SES (p=0.91) **(Table 1, Figure 2E)**. Covered stent struts on OCT axial images were frequently NIRF fibrin positive **(Supplementary Figure 2)**, consistent with prior studies demonstrating that early tissue coverage after DES placement is fibrin rich[10]. Histological assessment demonstrated that the NIRF signal colocalised with the fibrin, as detected by haematoxylin and eosin (H&E) and Carstairs' staining **(Figure 3)**. Histological evaluation revealed similar amounts of fibrin deposition among thin-strut and ultrathin-strut BP-SES.

CLINICAL OUTCOMES AFTER PCI WITH ULTRATHIN-STRUT VERSUS THIN-STRUT BP-SES

To assess the clinical relevance of these experimental findings, we performed a patient-level subgroup analysis of the BIOSTEMI[5] and BIOSCIENCE[11] randomised trials. In the overall pooled population from BIOSCIENCE and BIOSTEMI, we identified 2 subgroups of patients who were treated with either a single 3.0 mm (n=282, including 180 patients from BIOSCIENCE and 98 patients from BIOSTEMI) or 3.5 mm (n=222, including 120 patients from BIOSCIENCE and 102 patients from BIOSTEMI) BP-SES. In the overall combined population, we identified 4 subgroups of patients who

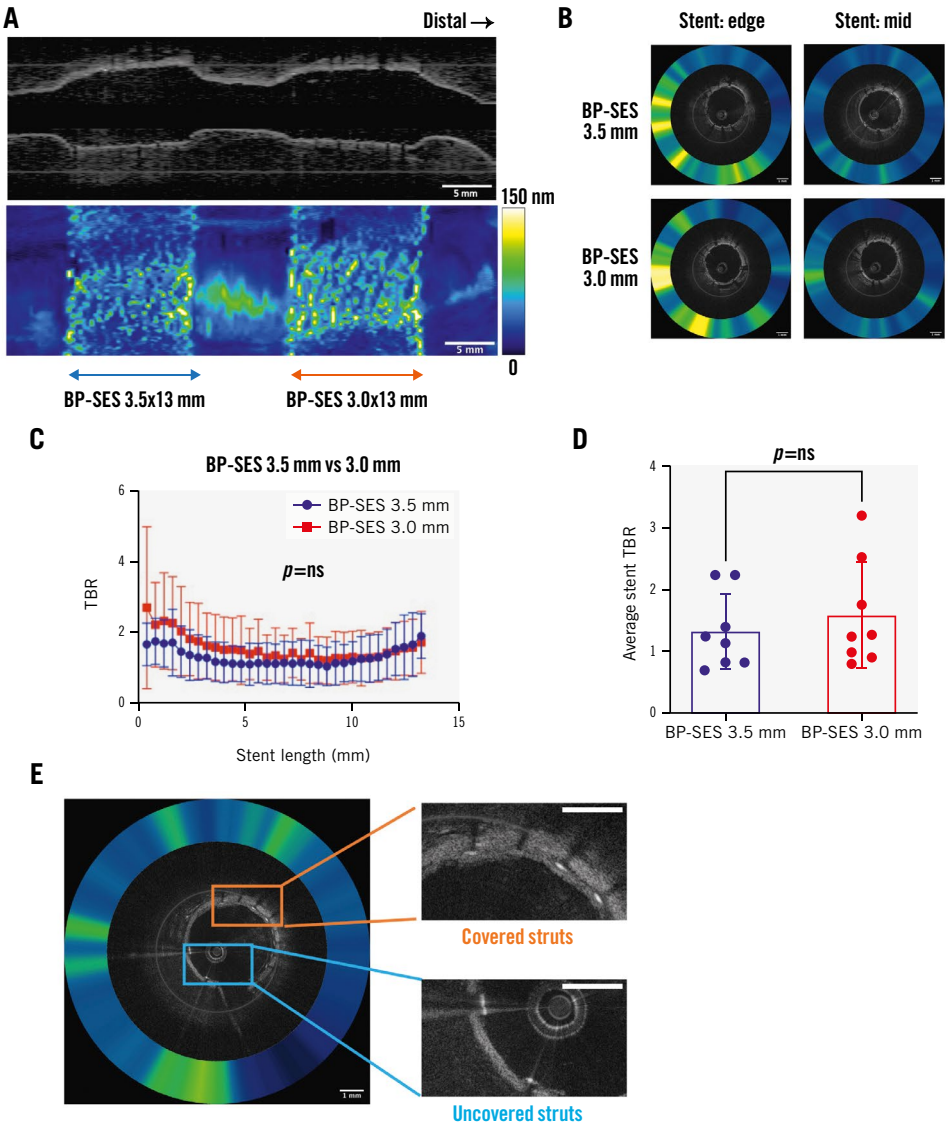

Figure 2. *Fibrin deposition on ultrathin-strut versus thin-strut BP-SES as assessed by NIRF-OCT molecular-structural imaging. In vivo two-dimensional fibrin NIRF-OCT map at day 7 post-stent implantation of non-overlapping 3.5 mm and 3.0 mm BP-SES. A) Long-axis NIRF image and (B) cross-sectional NIRF-OCT image, where the coregistered NIRF fibrin signal intensity is displayed as a quantitative ring around the OCT image. C) The NIRF fibrin signal plotted from the proximal to distal stent edge of BP-SES 3.5x13 mm and BP-SES 3.0x13 mm, averaged from the 8 rabbits (n=8 stents per group). D) The average of NIRF fibrin TBR across each 13 mm stent length. E) Representative NIRF-OCT images of covered and uncovered stent struts. Scale bar: 5 mm (long-axis NIRF image) or 1 mm (cross-sectional NIRF-OCT image). BP-SES: biodegradable-polymer sirolimus-eluting stent; NIRF: near-infrared fluorescence; ns: non-significant; OCT: optical coherence tomography; TBR: target-to-background ratio*

were treated with a single stent (either 3.0 mm or 3.5 mm diameter): BP-SES 3.5 mm (n=222), DP-EES 3.5 mm (n=233), BP-SES 3.0 mm (n=282), DP-EES 3.0 mm (n=260). TLF rates among groups were similar (p>0.05) **(Figure 4A)**. When comparing TLF rates for both stent platforms grouped into large diameter (3.5 mm, n=435) versus small diameter (3.0 mm, n=542), 1-year TLF rates remained similar for both stent platforms ($p_{interaction}$>0.05).

To specifically examine the difference in TLF rates as a function of stent strut thickness, we assessed differences between the ultrathin-strut BP-SES 3.0 mm and thin-strut BP-SES 3.5 mm groups. Differences in baseline clinical and procedural characteristics between treatment groups were controlled by the randomised allocation of the study stents **(Table 2)**. Compared to the thin-strut group, the ultrathin-strut group included a higher proportion of males, had higher rates of acute coronary syndrome, thrombus aspiration and direct stenting, and lower rates of bifurcation lesions. Medications, including dual antiplatelet therapy, were similar between the 2 groups at discharge, 30 days, and 1 year **(Supplementary Table 1)**. As a significant proportion of patients included in the present analysis had undergone

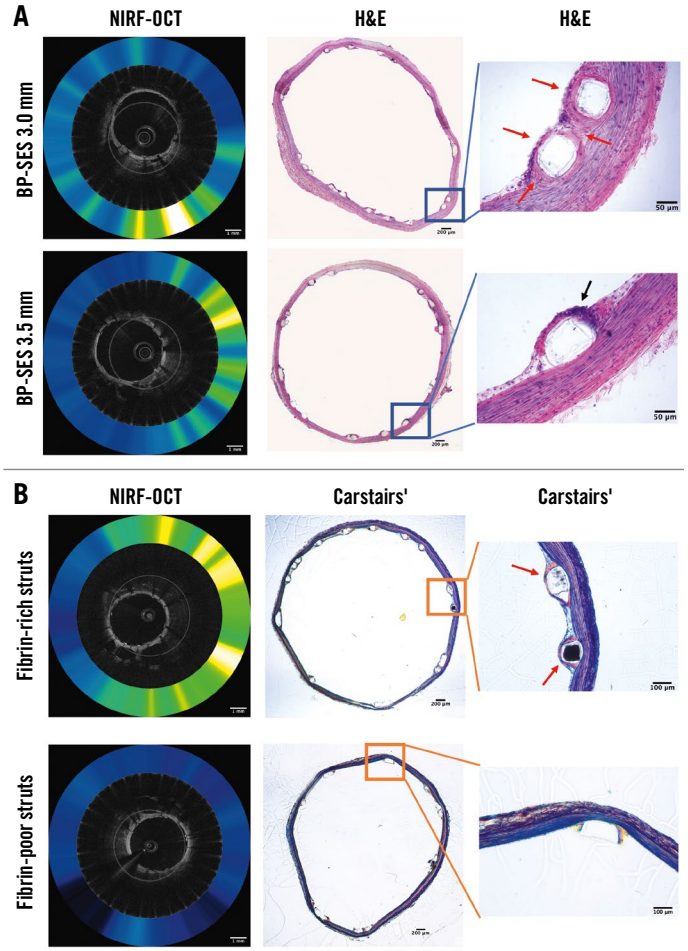

Figure 3. *Histological assessment of stent healing of ultrathin-strut (60 µm) and thin-strut (80 µm) BP-SES. A) Representative images of matched NIRF-OCT and haematoxylin and eosin (H&E) stained sections. B) Representative images of matched NIRF-OCT and Carstairs' histological images. Black arrows: inflammatory cells. Red arrows: fibrin deposition. Scale bar: 1 mm (NIRF-OCT image) or 200 µm, 100 µm, 50 µm (histological images). BP-SES: biodegradable-polymer sirolimus-eluting stent; NIRF-OCT: near-infrared fluorescence optical coherence tomography*

a previous PCI, a small number of patients underwent PCI for *de novo* coronary lesions that required implantation of an overlapping study stent with a previously implanted non-study stent **(Table 2)**.

We assessed the clinical outcomes at 30 days and 1 year between ultrathin-strut BP-SES and thin-strut BP-SES. Rates of TLF or the individual endpoints of cardiac death, target vessel myocardial infarction, or clinically indicated TLR did not differ significantly, at either 30 days or 1 year **(Table 3)**. Clinical outcomes from each individual trial (BIOSCIENCE and BIOSTEMI) are reported in **Supplementary Table 2** and **Supplementary Table 3**. Clinical outcomes at 1 year between ultrathin-strut BP-SES and thin-strut DP-EES were consistent when excluding patients (n=35) who had undergone PCI with either a single 3.0 mm or 3.5 mm stent for in-stent restenosis **(Supplementary Table 4)**.

Kaplan-Meier curves demonstrated similar rates of event accrual, with numerically higher TLF rates in the ultrathin strut BP-SES group at 30 days, but numerically lower event rates between 30 days and 1 year **(Figure 4B)**.

Discussion

Multiple studies demonstrate that ultrathin-strut DES exhibit improved clinical outcomes compared to thin-strut DES, driven by a reduction in clinically driven TLR[9,13,14]. However, the biophysical mechanisms underlying improved outcomes from ultrathin-strut DES remain uncertain. While ultrathin-strut thickness might underlie the observed clinical benefits, other features, such as the specific biodegradable polymer, antiproliferative drug/dose, and stent design, might also influence the observed benefits of BP-SES. To further investigate the specific feature of stent strut thickness, this integrative preclinical and clinical study compared the 60 µm and 80 µm BP-SES platforms utilising the same stent design, both experimentally and clinically. In summary, ultrathin-strut (60 µm) and thin-strut (80 µm) BP-SES exhibit similar preclinical stent healing profiles at subacute timepoints and demonstrate similar clinical outcomes at 30 days and 1 year.

Stent strut thickness has been long recognised as a critical feature that modulates stent healing. Kastrati et al first demonstrated improved clinical outcomes associated with

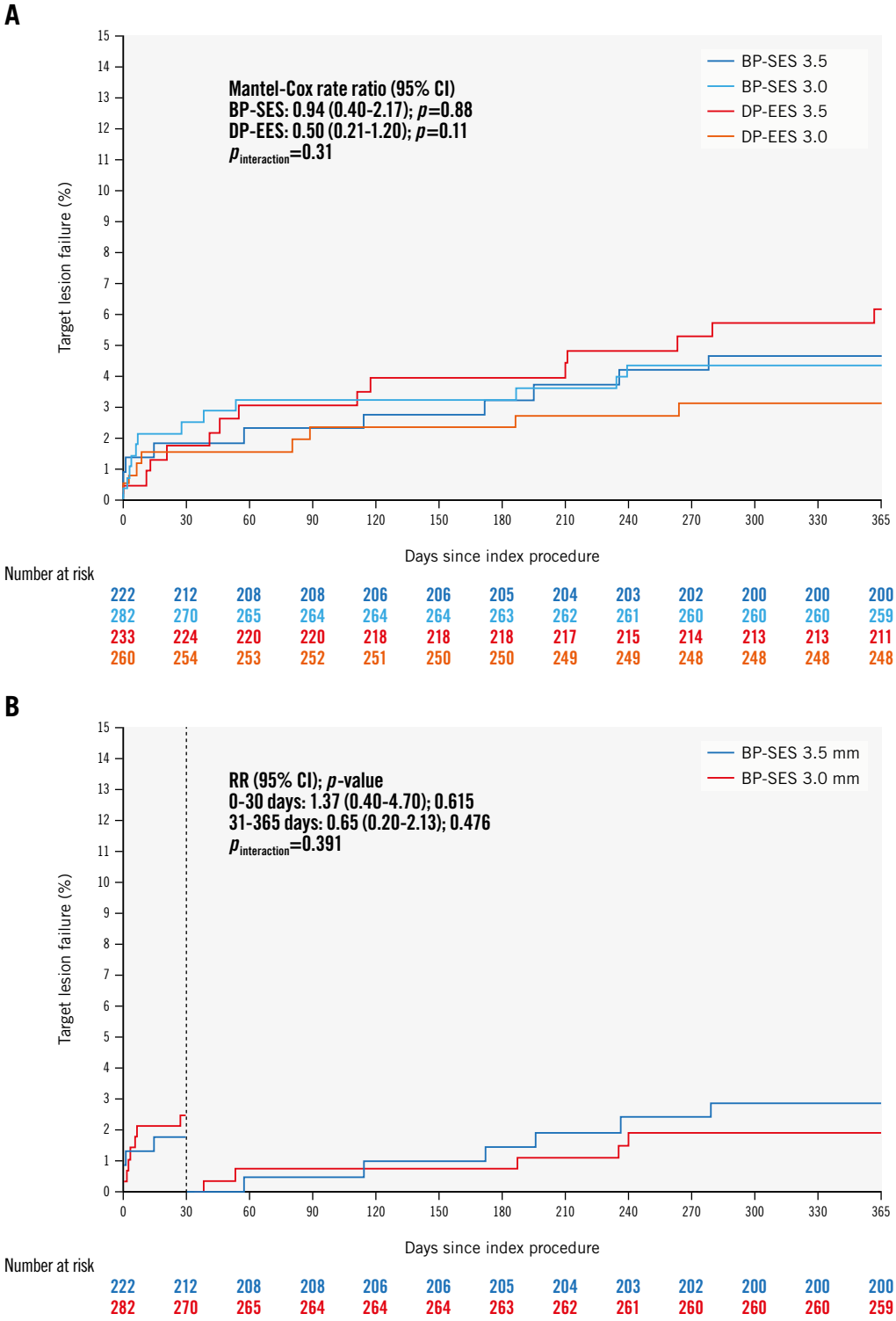

Figure 4. *Clinical outcomes of 504 pooled patients from the BIOSCIENCE and BIOSTEMI trials treated with either a 3.0 mm diameter or 3.5 mm diameter BP-SES or DP-EES. A) Time-to-event curves for target lesion failure (TLF) at 1 year of follow-up for all 4 groups. Blue line: thin-strut BP-SES (diameter 3.5 mm; strut thickness 80 µm); light blue line: ultrathin-strut BP-SES (diameter 3.0 mm; strut thickness 60 µm); red line: thin-strut DP-EES (diameter 3.5 mm; strut thickness 81 µm); orange line: thin-strut DP-EES (diameter 3.0 mm; strut thickness 81 µm). B) Time-to-event curves for 1-year TLF events in the two BP-SES groups, with a landmark set at 30 days. Blue line: thin-strut BP-SES (diameter 3.5 mm; strut thickness 80 µm); red line: ultrathin-strut BP-SES (diameter 3.0 mm; strut thickness 60 µm). BP-SES: biodegradable-polymer sirolimus-eluting stent; CI: confidence interval; DP-EES: durable-polymer everolimus-eluting stents; RR: risk ratio*

Table 2. Baseline clinical and procedural characteristics in the BP-SES groups from a pooled analysis of the BIOSCIENCE and BIOSTEMI trials.

	BP-SES 3.0 mm (60 µm) n=282	BP-SES 3.5 mm (80 µm) n=222	*p*-value
Age, years	64.6±11.4	62.9±11.9	0.096
Male	212 (75.2)	186 (83.8)	0.021
BMI, kg/m²	27.8±4.7	27.2±4.2	0.156
Diabetes mellitus	53 (18.8)	34 (15.3)	0.343
Insulin-dependent	20 (7.1)	10 (4.5)	0.258
Hypertension	168 (59.8)	123 (55.4)	0.363
Hypercholesterolaemia*	159 (56.8)	135 (60.8)	0.412
Current smoker	97 (34.9)	85 (38.6)	0.400
Prior MI	33 (11.7)	27 (12.2)	0.891
Previous PCI	56 (19.9)	39 (17.6)	0.567
Prior CABG	13 (4.6)	12 (5.4)	0.686
Prior stroke/TIA	8 (2.8)	4 (1.8)	0.563
Peripheral arterial disease	13 (4.6)	12 (5.4)	0.686
Chronic renal failure#	39 (14.6)	27 (12.6)	0.594
Left ventricular ejection fraction, %	53.9±12.1**	51.4±12.4##	0.064
Baseline medication			
Aspirin	104 (38.0)	77 (35.2)	0.573
Clopidogrel	21 (7.7)	11 (5.0)	0.272
Prasugrel	11 (4.0)	7 (3.2)	0.810
Ticagrelor	4 (1.5)	4 (1.8)	1.000
Any DAPT	30 (10.9)	18 (8.2)	0.360
Oral anticoagulation	15 (5.5)	8 (3.7)	0.394
Statin	96 (35.2)	80 (36.5)	0.777
ACE inhibitor	48 (17.6)	42 (19.2)	0.725
Beta blocker	98 (36.0)	61 (27.9)	0.065
Clinical presentation			
Chronic coronary syndrome	76 (27)	55 (24.8)	0.610
Acute coronary syndrome	206 (73)	167 (75.2)	0.012
Unstable angina	14 (6.8)	10 (6.0)	0.834
NSTEMI	55 (26.7)	24 (14.4)	0.005
STEMI	137 (66.5)	133 (79.6)	0.005
Target vessel location			0.239
Left main	1 (0.4)	3 (1.4)	0.325
Left anterior descending	141 (50.0)	105 (47.3)	0.590
Left circumflex	55 (19.5)	32 (14.4)	0.154
Right circumflex	82 (29.1)	80 (36.0)	0.103
Bypass graft	3 (1.1)	2 (0.9)	1.000
TIMI flow pre-PCI			0.091
0 or 1	99 (35.4)	93 (42.7)	0.115
2	46 (16.4)	23 (10.6)	0.067
3	135 (48.2)	102 (46.8)	0.786
TIMI flow post-PCI			0.510
2	6 (2.1)	3 (1.4)	0.738
3	275 (97.9)	219 (98.6)	0.738
Thrombus aspiration	61 (21.6)	71 (32.0)	0.011
In-stent restenosis	19 (6.7)	16 (7.2)	0.861
Chronic total occlusion	6 (2.1)	3 (1.4)	0.738
Bifurcation lesion	42 (14.9)	18 (8.1)	0.026
Total stent length, mm	22.00±6.92	21.54±6.80	0.460
Maximum pressure, atm	13.46±3.18	13.28±3.36	0.527
Overlapping stents	2 (0.7)	1 (0.5)	1.000
Direct stenting	67 (23.8)	73 (32.9)	0.027
Post-dilatation	136 (48.2)	94 (42.3)	0.208

Data are expressed as mean±SD, n (%) or sample size [n]. *total cholesterol >5.0 mmol or 190 mg/dl or requiring treatment; #glomerular filtration rate <60 ml/min; **n=200; ##n=143. ACE: angiotensin-converting enzyme; BMI: body mass index; BP-SES: biodegradable-polymer sirolimus-eluting stents; CABG: coronary artery bypass grafting; DAPT: dual antiplatelet therapy; MI: myocardial infarction; NSTEMI: non-ST-segment elevation myocardial infarction; PCI: percutaneous coronary intervention; STEMI: ST-segment elevation myocardial infarction; TIA: transient ischaemic attack; TIMI: Thrombolysis in Myocardial Infarction

Table 3. Clinical outcomes of BP-SES at 30 days and 1 year of follow-up.

	BP-SES 3.0 mm (60 µm) N=222	BP-SES 3.5 mm (80 µm) N=222	Rate ratio (95% CI)	*p*-value
At 30 days				
Target lesion failure*	7 (2.5)	4 (1.8)	1.37 (0.40-4.70)	0.615
Cardiac death	5 (1.8)	1 (0.5)	3.95 (0.46-34.03)	0.176
Target vessel MI	1 (0.4)	3 (1.4)	0.26 (0.03-2.53)	0.211
Clinically indicated TLR	2 (0.7)	1 (0.5)	1.58 (0.14-17.51)	0.708
All-cause death	5 (1.8)	2 (0.9)	1.97 (0.38-10.17)	0.409
Myocardial infarction (any)	1 (0.4)	3 (1.4)	0.26 (0.03-2.53)	0.211
Revascularisation (any)	4 (1.4)	1 (0.5)	3.16 (0.35-28.39)	0.277
TLR (any)	2 (0.7)	1 (0.5)	1.58 (0.14-17.51)	0.708
TVR (any)	2 (0.7)	1 (0.5)	1.58 (0.14-17.51)	0.708
Clinically indicated TVR	2 (0.7)	1 (0.5)	1.58 (0.14-17.51)	0.708
Stroke (any)	0 (0.0)	2 (0.9)	0.34 (0.05-2.28)	0.325
Target vessel failure**	7 (2.5)	4 (1.8)	1.37 (0.40-4.70)	0.615
Cardiac death, or MI (any)	6 (2.1)	4 (1.8)	1.17 (0.33-4.18)	0.804
Death, MI, or any revascularisation	9 (3.2)	5 (2.3)	1.41 (0.47-4.22)	0.536
Definite stent thrombosis	1 (0.4)	1 (0.5)	0.79 (0.05-12.72)	0.865
Definite/probable stent thrombosis	4 (1.4)	4 (1.8)	0.78 (0.19-3.14)	0.728
At 1 year				
Target lesion failure*	12 (4.3)	10 (4.7)	0.94 (0.40-2.17)	0.882
Cardiac death	7 (2.5)	4 (1.9)	1.38 (0.40-4.71)	0.606
Target vessel MI	2 (0.7)	5 (2.3)	0.31 (0.06-1.62)	0.142
Clinically indicated TLR	5 (1.8)	5 (2.4)	0.79 (0.23-2.73)	0.708
All-cause death	9 (3.2)	8 (3.7)	0.89 (0.34-2.30)	0.803
Myocardial infarction (any)	3 (1.1)	8 (3.7)	0.29 (0.08-1.10)	0.053
Revascularisation (any)	13 (4.8)	7 (3.3)	1.49 (0.59-3.73)	0.396
TLR (any)	6 (2.2)	5 (2.4)	0.95 (0.29-3.12)	0.933
TVR (any)	8 (3.0)	5 (2.4)	1.27 (0.41-3.89)	0.675
Clinically indicated TVR	7 (2.6)	5 (2.4)	1.11 (0.35-3.51)	0.857
Stroke (any)	1 (0.4)	3 (1.4)	0.26 (0.03-2.54)	0.212
Target vessel failure**	15 (5.4)	10 (4.7)	1.18 (0.53-2.62)	0.690
Cardiac death, or MI (any)	10 (3.6)	11 (5.1)	0.71 (0.30-1.67)	0.427
Death, MI, or any revascularisation	22 (8.0)	16 (7.4)	1.08 (0.57-2.07)	0.805
Definite stent thrombosis	2 (0.7)	3 (1.4)	0.52 (0.09-3.15)	0.473
Definite/probable stent thrombosis	5 (1.8)	6 (2.8)	0.65 (0.20-2.14)	0.476

Data are presented as number of first events (% cumulative incidence) from Kaplan-Meier estimate. Rate ratios, 95% confidence intervals (CI), and log-rank p-values are from Mantel-Cox regressions. *Composite of cardiac death: target vessel myocardial infarction, and clinically indicated TLR. **Composite of cardiac death, any myocardial infarction, and any target vessel revascularisation. BP-SES: biodegradable-polymer sirolimus-eluting stents; MI: myocardial infarction; TLR: target lesion revascularisation; TVR: target vessel revascularisation

a reduction of strut thickness[4]. Soucy et al showed that a lower stent strut thickness improved strut tissue coverage following stent implantation in rabbits[15]. In addition, reductions in stent strut thickness of second-generation DES (typically 81 µm stent strut thickness) were further associated with improved clinical outcomes, as compared to thicker-strut first-generation DES (132-140 µm strut thickness)[16]. This finding likely motivated the development of ultrathin-strut stents, including a BP-SES platform with a strut thickness of 60 µm for a 3.0 mm stent diameter[17]. Yet the specific parameter of ultrathin-strut thickness on stent healing and clinical outcomes has not been rigorously investigated.

The experimental arm of this study showed similar day 7 subacute stent healing and stent tissue coverage between BP-SES groups in rabbits. The day 7 rabbit timepoint was chosen specifically to mirror the ~1 month timepoint in humans[18], when the early benefits of BP-SES emerged in the BIOSTEMI trial[5]. A strength of the experimental design was to vary the stent strut thickness without changing the antiproliferative drug (sirolimus), biodegradable polymer (poly-L-lactic acid [PLLA]), or stent design (3 connectors, 8 crowns

at the end), while maintaining similar stent expansion ratios for the 2 platforms **(Table 1)**. Consistent with an earlier preclinical stent fibrin imaging study[10], we found that day 7 stent tissue coverage assessed by OCT was fibrin rich **(Figure 2, Supplementary Figure 2)**, indicating an unhealed state in the subacute phase after stenting. These findings further reinforce the value of NIRF fibrin molecular imaging, as standalone OCT appears insufficient for understanding the pathogenicity of early stent tissue coverage, namely whether a covered stent strut is covered by fibrin (prothrombotic, unhealed) or endothelial cells (antithrombotic, healed)[10].

To determine the clinical impact of ultrathin-strut thickness, we investigated whether clinical outcomes differed between ultrathin-strut BP-SES and thin-strut BP-SES in a pooled analysis of individual patient data from the BIOSCIENCE[11] and BIOSTEMI[5] randomised trials. These two trials compared BP-SES versus DP-EES in patients undergoing PCI. In a prespecified subgroup analysis from the BIOSCIENCE trial which included 407 ST-elevation myocardial infarction (STEMI) patients, BP-SES exhibited significantly lower 1-year TLF rates compared to DP-EES[19]. In the dedicated BIOSTEMI trial that randomised 1,300 STEMI patients 1:1 to treatment with BP-SES or DP-EES[5], BP-SES demonstrated superior outcomes, compared to the DP-EES, with a 41% reduction in the risk of TLF at 1 year of follow-up, driven by reductions in clinically driven TLR. The clinical benefits of BP-SES over DP-EES emerged within the first month after PCI, which motivated the current rabbit day 7 timepoint analysis. However, consistent with our preclinical results, we found no significant differences in the 30-day and 1-year TLF rates between ultrathin-strut BP-SES and thin-strut BP-SES **(Figure 4B)**. In addition, while prior studies suggest that TLF rates might be higher in smaller-diameter vessels[20], which could affect the current results, we observed no statistically significant differences in 1-year TLF rates for small-diameter versus large-diameter stents in our pooled RCT analysis, for either BP-SES or DP-EES **(Figure 4A)**. These results are also consistent with a recent study that compared TLF rates between multistent and single-stent lesions for BP-SES and DP-EES[21]. However, no specific analysis was performed between ultrathin-strut and thin-strut BP-SES.

From a translational imaging perspective, intracoronary NIRF-OCT has already been performed in patients with coronary artery disease to detect NIR autofluorescence (NIRAF)[22], a high-risk plaque feature reflecting intraplaque haemorrhage, and ceroid derived from oxidative stress[23-25]. From an imaging agent standpoint, the fibrin-targeted NIRF molecular imaging agent is peptide based[10], and a magnetic resonance imaging analogue has already been tested clinically[26]. Therefore, clinical intracoronary NIRF-OCT fibrin molecular imaging appears feasible to unravel the mechanisms of DES healing, and potentially to detect the risk of stent thrombosis.

Limitations

This study has limitations. Experimentally, stent healing was assessed in normal rather than atheroma-bearing rabbit arteries, consistent with prior preclinical stent healing studies[27] and, thus, may not recapitulate all features of stent healing in patients. In addition, stent deployment at day 0 was assessed with only IVUS and not OCT. Although OCT is preferred for assessing post-stenting malapposition, in a rabbit, OCT is more invasive than IVUS, because it requires a separate arterial access via the carotid artery cutdown to allow for balloon occlusion and blood clearance. Considering the degree of invasiveness, which could risk animal death, and the need to preserve an arterial access for the day 7 primary endpoint, we deferred OCT on day 0 and performed IVUS pullback only. While DP-EES were not experimentally studied for stent healing, the focus of this study was to assess the impact of the specific parameter of strut thickness between otherwise similarly constructed stents. We could not compare preclinical ultrathin-strut versus thin-strut stent healing in smaller vessels (e.g., 2.5 mm diameter) due to the risk of dissection with the larger 3.5 mm platform, and, intentionally, the clinical analysis matched the 3.0 mm/3.5 mm preclinical framework. Another limitation was that we could not specifically compare healing of the same diameter stent with thin-strut versus ultrathin-strut thickness in large arteries (e.g., a 3.5 mm BP-SES with 60 µm vs a 3.5 mm BP-SES with 80 µm strut thickness), nor in smaller arteries (e.g., a 2.5 mm BP-SES with 60 µm vs a 2.5 mm BP-SES with 80 µm strut thickness) that typically have poorer outcomes[20], as the manufacturer only provides 1 strut thickness for a given stent diameter. The latter inability to compare small-diameter vessel healing and outcomes between ultrathin-strut and thin-strut BP-SES remains a limitation, as it is still possible that ultrathin-strut thickness could confer an advantage in smaller-diameter arteries. However, it is also noteworthy that for 3.0 mm diameter vessels, ultrathin-strut BP-SES showed numerically higher event rates than thin-strut DP-EES **(Figure 4A)**, again supporting the concept that ultrathin-strut thickness may not confer improved clinical outcomes in large vessels. The day 7 timepoint for preclinical assessment was chosen based on the BIOSTEMI trial showing benefits emerging by 30 days post-PCI; later timepoints might reveal differences in stent healing, although prior preclinical data shows smaller differences in stent coverage and fibrin deposition at later timepoints such as day 28[10,27]. While the NIRF-OCT fibrin/coverage imaging protocol was focused on assessing subacute stent healing, separate preclinical studies might evaluate neointimal hyperplasia and neoatherosclerosis at later timepoints, features that could also underlie the improved TLF rates noted with BP-SES. In the BIOSTEMI and BIOSCIENCE trials, patients were not randomised to receive thin-strut versus ultrathin-strut stents of otherwise similar stent designs, and were not randomised based on the presence or absence of a bifurcation lesion. Finally, the present analysis included a small number of patients (n=3) who underwent PCI with a single ultrathin-strut BP-SES that overlapped a previously implanted non-study stent. While PCI with overlapping stents may induce different arterial wall response patterns than those caused by single stent implantation, the inclusion of a limited number of patients with overlapping stents in the present analysis is unlikely to have influenced the overall study results.

Conclusions

In conclusion, this experimental and clinical study found similar early stent healing patterns and 30-day and 1-year clinical outcomes for ultrathin-strut and thin-strut BP-SES **(Central illustration)**. These findings provide evidence that features beyond ultrathin-strut thickness may underlie the observed benefits of BP-SES compared to current DP-EES[9,13]. Furthermore, we

Preclinical and clinical investigation of ultrathin-strut versus thin-strut BP-SES shows similar early healing and 1-year clinical outcomes.

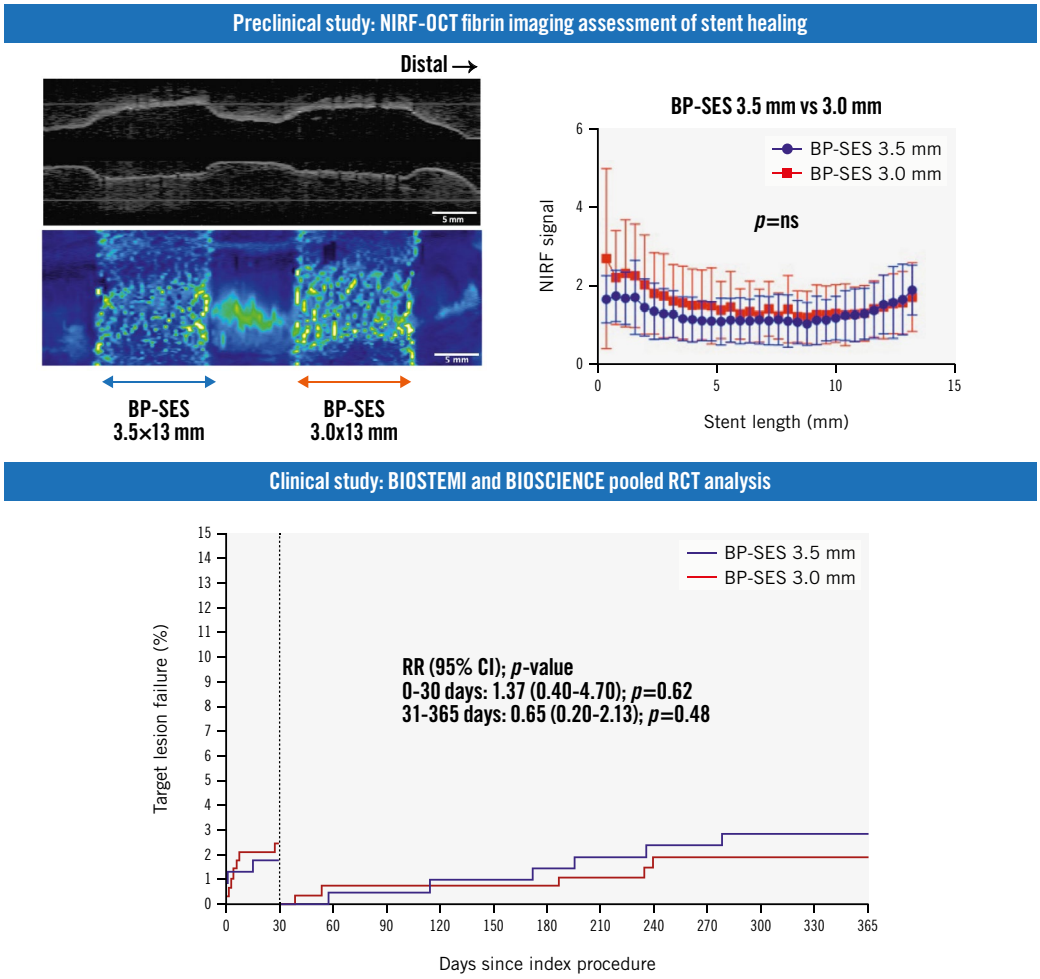

Ryutaro Ikegami *et al.* • *EuroIntervention* 2024;20:e669-e680 • DOI: 10.4244/EIJ-D-23-00563

BP-SES: biodegradable-polymer sirolimus-eluting stent; CI: confidence interval; NIRF: near-infrared fluorescence; ns: non-significant; OCT: optical coherence tomography; RCT: randomised controlled trial; RR: risk ratio

surmise that further reduction of stent strut thickness beyond 60 µm may not offer additional clinical advantages, given the current results and potential for lower radial strength. However, further investigation of ultrathin-strut DES in smaller arteries, which have higher event rates in general[20], may be needed, as the lower ratio of strut thickness to stent diameter is more favourable for ultrathin-strut DES. Other stent features to investigate and refine in the ongoing quest to improve DES outcomes may include stent design, novel stent metals and polymers, and antiproliferative drug candidates. Overall, based on the current data, the potential clinical benefits observed with BP-SES may be independent of stent strut thickness.

Authors' affiliations

1. Division of Cardiology, Cardiovascular Research Center, Massachusetts General Hospital, Boston, MA, USA; 2. Department of Cardiovascular Biology and Medicine, Niigata University Graduate School of Medical and Dental Sciences, Niigata, Japan; 3. Wellman Center for Photomedicine, Harvard Medical School and Massachusetts General Hospital, Boston, MA, USA; 4. Department of Cardiology, Geneva University Hospitals, Geneva, Switzerland; 5. Bern University Hospital, Bern, Switzerland; 6. Masonic Medical Research Institute, Utica, NY, USA; 7. Center for Systems Biology, Massachusetts General Hospital, Boston, MA, USA; 8. Klink Fur Herz- und Kreislauferkrankungen, Deutsches Herzzentrum München, Technische Universitat München, München, Germany; 9. DZHK (German Centre for Cardiovascular Research), partner site Munich Heart Alliance, München, Germany; 10. Department of Medicine, Division of Cardiology, University of Toronto, Toronto, Canada; 11. Piedmont Heart Institute, Atlanta, GA, USA; 12. Harvard-Massachusetts Institute of

Technology Health Sciences and Technology, Cambridge, MA, USA; 13. Institute for Medical Engineering and Science, Massachusetts Institute of Technology, Cambridge, MA, USA; 14. Cardiovascular Division, Brigham and Women's Hospital, Boston, MA, USA; 15. CTU Bern, Bern University, Bern, Switzerland

Funding

The following NIH grants provided funding for our study: R01HL137913, R01HL144550, R01HL150538, R01HL165453. The NIRF-OCT system was developed in part under R01HL093717 to Guillermo J. Tearney. Elazer R. Edelman was funded in part by NIH R01HL161069. FTP11-CyAm7 was synthesised under Halfond-Weil fellowship and AHA953662 to Khanh Ha. The BIOSCIENCE and BIOSTEMI trials were supported by dedicated grants from Biotronik.

Conflict of interest statement

F.A. Jaffer – sponsored research: Canon, Siemens, Shockwave Medical, Teleflex, Amarin, Mercator, Boston Scientific, HeartFlow, and Neovasc; consultant/speaker fees: Boston Scientific, Siemens, Magenta Medical, Philips, Biotronik, Terumo, Mercator, Abiomed, Medtronic, and FastWave; and equity interest: Intravascular Imaging Inc, DurVena, and FastWave. G.J. Tearney – sponsored research: Merck Sharp & Dohme and Canon; catheter components: Terumo; consultant: Samsung; consultant and board member and holds equity: SpectraWAVE. Massachusetts General Hospital – licensing arrangements: Terumo, Canon, SpectraWAVE, for which G.J. Tearney and F.A. Jaffer have the right to receive royalties. J.F. Iglesias – research grant to the institution and personal fees from Biotronik during the conduct of the BIOSTEMI trial; research grants to the institution from Abbott, AstraZeneca, Biosensors, Biotronik, Concept Medical, Philips Volcano, and Terumo Corp., outside of the submitted work; personal fees from AstraZeneca, Biotronik, Bristol-Myers Squibb, MedAlliance, Novartis, Terumo, Medtronic, Philips Volcano, and Cordis, outside the submitted work; consultant for Biotronik, Cordis, Medtronic, ReCor Medical, and Terumo Corp. T. Pilgrim – received research grants to the institution from Biotronik, Boston Scientific, and Edwards Lifesciences; and speaker fees/consultancy from Biotronik, Boston Scientific, Edwards Lifesciences, Abbott, Medtronic, and HighLife SAS. D. Heg – employed by CTU Bern, University of Bern, which has a staff policy of not accepting honoraria or consultancy fees; however, CTU Bern is involved in the design, conduct, or analysis of clinical studies funded by not-for-profit and for-profit organisations; in particular, pharmaceutical and medical device companies provide direct funding to some of these studies; for an up-to-date list of CTU Bern's conflicts of interest see https://www.ctu.unibe.ch/research_projects/declaration_of_interest/index_eng.html. D.E. Kandzari – institutional research/grant support from Biotronik, Boston Scientific, CSI, Medtronic, OrbusNeich, and Teleflex; and personal consulting honoraria from CSI, Medtronic, and Orchestra BioMed. The other authors have no conflicts of interest to declare.

References

1. Piccolo R, Bonaa KH, Efthimiou O, Varenne O, Baldo A, Urban P, Kaiser C, Remkes W, Räber L, de Belder A, van 't Hof AWJ, Stankovic G, Lemos PA, Wilsgaard T, Reifart J, Rodriguez AE, Ribeiro EE, Serruys PWJC, Abizaid A, Sabaté M, Byrne RA, de la Torre Hernandez JM, Wijns W, Jüni P, Windecker S, Valgimigli M; Coronary Stent Trialists' Collaboration. Drug-eluting or bare-metal stents for percutaneous coronary intervention: a systematic review and individual patient data meta-analysis of randomised clinical trials. *Lancet*. 2019;393:2503-10.

2. Baber U, Mehran R, Sharma SK, Brar S, Yu J, Suh JW, Kim HS, Park SJ, Kastrati A, de Waha A, Krishnan P, Moreno P, Sweeny J, Kim MC, Suleman J, Pyo R, Wiley J, Kovacic J, Kini AS, Dangas GD. Impact of the everolimus-eluting stent on stent thrombosis: a meta-analysis of 13 randomized trials. *J Am Coll Cardiol*. 2011;58:1569-77.

3. Kolandaivelu K, Swaminathan R, Gibson WJ, Kolachalama VB, Nguyen-Ehrenreich KL, Giddings VL, Coleman L, Wong GK, Edelman ER. Stent thrombogenicity early in high-risk interventional settings is driven by stent design and deployment and protected by polymer-drug coatings. *Circulation*. 2011;123:1400-9.

4. Kastrati A, Mehilli J, Dirschinger J, Dotzer F, Schühlen H, Neumann FJ, Fleckenstein M, Pfafferott C, Seyfarth M, Schömig A. Intracoronary stenting and angiographic results: strut thickness effect on restenosis outcome (ISAR-STEREO) trial. *Circulation*. 2001;103:2816-21.

5. Iglesias JF, Muller O, Heg D, Roffi M, Kurz DJ, Moarof I, Weilenmann D, Kaiser C, Tapponnier M, Stortecky S, Losdat S, Eeckhout E, Valgimigli M, Odutayo A, Zwahlen M, Jüni P, Windecker S, Pilgrim T. Biodegradable polymer sirolimus-eluting stents versus durable polymer everolimus-eluting stents in patients with ST-segment elevation myocardial infarction (BIOSTEMI): a single-blind, prospective, randomised superiority trial. *Lancet*. 2019;394:1243-53.

6. Pilgrim T, Muller O, Heg D, Roffi M, Kurz DJ, Moarof I, Weilenmann D, Kaiser C, Tapponnier M, Losdat S, Eeckhout E, Valgimigli M, Jüni P, Windecker S, Iglesias JF. Biodegradable- Versus Durable-Polymer Drug-Eluting Stents for STEMI: Final 2-Year Outcomes of the BIOSTEMI Trial. *JACC Cardiovasc Interv*. 2021;14:639-48.

7. Iglesias JF, Muller O, Losdat S, Roffi M, Kurz DJ, Weilenmann D, Kaiser C, Valgimigli M, Windecker S, Pilgrim T. Ultrathin-Strut Versus Thin-Strut Drug-Eluting Stents for Primary PCI: A Subgroup Analysis of the BIOSTEMI Randomized Trial. *JACC Cardiovasc Interv*. 2020;13:2314-6.

8. Kandzari DE, Mauri L, Koolen JJ, Massaro JM, Doros G, Garcia-Garcia HM, Bennett J, Roguin A, Gharib EG, Cutlip DE, Waksman R; BIOFLOW V Investigators. Ultrathin, bioresorbable polymer sirolimus-eluting stents versus thin, durable polymer everolimus-eluting stents in patients undergoing coronary revascularisation (BIOFLOW V): a randomised trial. *Lancet*. 2017;390:1843-52.

9. Madhavan MV, Howard JP, Naqvi A, Ben-Yehuda O, Redfors B, Prasad M, Shahim B, Leon MB, Bangalore S, Stone GW, Ahmad Y. Long-term follow-up after ultrathin vs. conventional 2nd-generation drug-eluting stents: a systematic review and meta-analysis of randomized controlled trials. *Eur Heart J*. 2021;42:2643-54.

10. Hara T, Ughi GJ, McCarthy JR, Erdem SS, Mauskapf A, Lyon SC, Fard AM, Edelman ER, Tearney GJ, Jaffer FA. Intravascular fibrin molecular imaging improves the detection of unhealed stents assessed by optical coherence tomography in vivo. *Eur Heart J*. 2017;38:447-55.

11. Pilgrim T, Heg D, Roffi M, Tüller D, Muller O, Vuilliomenet A, Cook S, Weilenmann D, Kaiser C, Jamshidi P, Fahrni T, Moschovitis A, Noble S, Eberli FR, Wenaweser P, Jüni P, Windecker S. Ultrathin strut biodegradable polymer sirolimus-eluting stent versus durable polymer everolimus-eluting stent for percutaneous coronary revascularisation (BIOSCIENCE): a randomised, single-blind, non-inferiority trial. *Lancet*. 2014;384:2111-22.

12. Joner M, Finn AV, Farb A, Mont EK, Kolodgie FD, Ladich E, Kutys R, Skorija K, Gold HK, Virmani R. Pathology of drug-eluting stents in humans: delayed healing and late thrombotic risk. *J Am Coll Cardiol*. 2006;48:193-202.

13. Zhu P, Zhou X, Zhang C, Li H, Zhang Z, Song Z. Safety and efficacy of ultrathin strut biodegradable polymer sirolimus-eluting stent versus durable polymer drug-eluting stents: a meta-analysis of randomized trials. *BMC Cardiovasc Disord*. 2018;18:170.

14. Iglesias JF, Degrauwe S, Cimci M, Chatelain Q, Roffi M, Windecker S, Pilgrim T. Differential Effects of Newer-Generation Ultrathin-Strut Versus Thicker-Strut Drug-Eluting Stents in Chronic and Acute Coronary Syndromes. *JACC Cardiovasc Interv*. 2021;14:2461-73.

15. Soucy NV, Feygin JM, Tunstall R, Casey MA, Pennington DE, Huibregtse BA, Barry JJ. Strut tissue coverage and endothelial cell coverage: a comparison between bare metal stent platforms and platinum chromium stents with and without everolimus-eluting coating. *EuroIntervention*. 2010;6:630-7.

16. Gada H, Kirtane AJ, Newman W, Sanz M, Hermiller JB, Mahaffey KW, Cutlip DE, Sudhir K, Hou L, Koo K, Stone GW. 5-year results of a randomized comparison of XIENCE V everolimus-eluting and TAXUS paclitaxel-eluting stents: final results from the SPIRIT III trial (clinical evaluation of the XIENCE V everolimus eluting coronary stent system in the treatment of patients with de novo native coronary artery lesions). *JACC Cardiovasc Interv*. 2013;6:1263-6.

17. Iglesias JF, Roffi M, Degrauwe S, Secco GG, Aminian A, Windecker S, Pilgrim T. Orsiro cobalt-chromium sirolimus-eluting stent: present and future perspectives. *Expert Rev Med Devices*. 2017;14:773-88.

18. Virmani R, Kolodgie FD, Farb A, Lafont A. Drug eluting stents: are human and animal studies comparable? *Heart*. 2003;89:133-8.

19. Pilgrim T, Piccolo R, Heg D, Roffi M, Tüller D, Vuilliomenet A, Muller O, Cook S, Weilenmann D, Kaiser C, Jamshidi P, Khattab AA, Taniwaki M, Rigamonti F, Nietlispach F, Blöchlinger S, Wenaweser P, Jüni P, Windecker S. Biodegradable polymer sirolimus-eluting stents versus durable polymer everolimus-eluting stents for primary percutaneous coronary revascularisation of acute myocardial infarction. *EuroIntervention*. 2016;12:e1343-54.

20. Sanz-Sánchez J, Chiarito M, Gill GS, van der Heijden LC, Piña Y, Cortese B, Alfonso F, von Birgelen C, Gil JLD, Waksman R, Garcia-Garcia HM. Small Vessel Coronary Artery Disease: Rationale for Standardized Definition and Critical Appraisal of the Literature. *J Soc Cardiovasc Angiogr Interv*. 2022;1:100403.

21. Häner JD, Rohla M, Losdat S, Iglesias JF, Muller O, Eeckhout E, Kurz D, Weilenmann D, Kaiser C, Tapponnier M, Roffi M, Heg D, Windecker S, Pilgrim T. Ultrathin-strut vs thin-strut drug-eluting stents for multi and single-stent lesions: A lesion-level subgroup analysis of 2 randomized trials. *Am Heart J*. 2023;263:73-84.

22. Ughi GJ, Verjans J, Fard AM, Wang H, Osborn E, Hara T, Mauskapf A, Jaffer FA, Tearney GJ. Dual modality intravascular optical coherence tomography (OCT) and near-infrared fluorescence (NIRF) imaging: a fully automated algorithm for the distance-calibration of NIRF signal intensity for quantitative molecular imaging. *Int J Cardiovasc Imaging*. 2015;31:259-68.

23. Htun NM, Chen YC, Lim B, Schiller T, Maghzal GJ, Huang AL, Elgass KD, Rivera J, Schneider HG, Wood BR, Stocker R, Peter K. Near-infrared autofluorescence induced by intraplaque hemorrhage and heme degradation as marker for high-risk atherosclerotic plaques. *Nat Commun*. 2017;8:75.

24. Albaghdadi MS, Ikegami R, Kassab MB, Gardecki JA, Kunio M, Chowdhury MM, Khamis R, Libby P, Tearney GJ, Jaffer FA. Near-Infrared Autofluorescence in Atherosclerosis Associates With Ceroid and Is Generated by Oxidized Lipid-Induced Oxidative Stress. *Arterioscler Thromb Vasc Biol*. 2021;41:e385-98.

25. Kunio M, Gardecki JA, Watanabe K, Nishimiya K, Verma S, Jaffer FA, Tearney GJ. Histopathological correlation of near infrared autofluorescence in human cadaver coronary arteries. *Atherosclerosis*. 2022;344:31-9.

26. Spuentrup E, Botnar RM, Wiethoff AJ, Ibrahim T, Kelle S, Katoh M, Ozgun M, Nagel E, Vymazal J, Graham PB, Günther RW, Maintz D. MR imaging of thrombi using EP-2104R, a fibrin-specific contrast agent: initial results in patients. *Eur Radiol*. 2008;18:1995-2005.

27. Finn AV, Nakazawa G, Joner M, Kolodgie FD, Mont EK, Gold HK, Virmani R. Vascular responses to drug eluting stents: importance of delayed healing. *Arterioscler Thromb Vasc Biol*. 2007;27:1500-10.

Supplementary data

Supplementary Appendix 1. Methods.

Supplementary Table 1. Medication at discharge, 30 days and 1 year of follow-up.

Supplementary Table 2. Clinical outcomes of BIOSTEMI only at 30 days and 1 year of follow-up.

Supplementary Table 3. Clinical outcomes of BIOSCIENCE only at 30 days and 1 year of follow-up.

Supplementary Table 4. Clinical outcomes at 1 year in patients that did not present with in-stent restenosis.

Supplementary Figure 1. *Ex vivo* NIRF molecular imaging of fibrin deposition on BP-SES stents.

Supplementary Figure 2. NIRF-OCT fibrin assessment of uncovered and covered stent struts.

The supplementary data are published online at: https://eurointervention.pcronline.com/doi/10.4244/EIJ-D-23-00563

Supplementary data

Supplementary Appendix 1. Methods.

In vivo rabbit study of ultrathin-strut versus thin-strut BP-SES stent healing

The Institutional Animal Care and Use Committee at Massachusetts General Hospital approved all animal studies (2013N000015). The study design is illustrated in Figure 1. New Zealand white rabbits (N=8, Millbrook Farms, Amherst, MA) were anesthetized with intramuscular ketamine (35mg/kg)/xylazine (5mg/kg) mixture and maintained by inhaled isoflurane (1-5% vol/vol). A 4Fr sheath was inserted into the right iliac artery and heparin (150 units/kg) and nitroglycerin (50ug) were administered via the sheath. A baseline iodinated contrast angiogram was performed. A 0.014 inch guidewire was introduced into the abdominal aorta and an intravascular ultrasound (IVUS) pullback was performed from the renal arteries to the iliac bifurcation to measure the vessel diameter. Next balloon injury with coronary angioplasty balloon was performed targeting a balloon-to-artery ratio of 1.1-1.2 in an aortic segment prior to stenting. Then a BP-SES 3.5mm stent consisting of a thin-strut platform (80 □m, Orsiro, Biotronik, Germany) in the proximal abdominal aorta and a BP-SES 3.0mm stent of the same stent platform except for construction with ultrathin-stent struts (60 □m, Orsiro) were deployed in the distal abdominal aorta with appropriate pressure to achieve apposition. The Orsiro BP-SES consists of a cobalt chromium alloy with two different stent thicknesses. For stent diameters ≤3.0 mm, the stent strut thickness and width are 60 □m and 75 □m, respectively. For stent diameters ≥3.5 mm, the stent strut thickness and width are 80 □m and 85 □m, respectively. Stents are coated with an amorphous silicon carbide surface layer and covered by a biodegradable poly-L-lactic acid polymer on the abluminal side. The polymer releases sirolimus over 12-14 weeks, with complete degradation observed by ~24 months[17].

The stents were placed in nonoverlapping fashion and separated by approximately 10 mm in the infrarenal aorta. To archive a stent-to-artery ratio of 1.1-1.2, postdilatation of each stent using a non-compliant coronary angioplasty balloon (3.5-3.75mm diameter) was performed with the appropriate pressure. IVUS was performed post-stent deployment to assess acute stent expansion and for the presence of arterial dissection. Rabbits received aspirin 40mg and clopidogrel 75mg from one day before stenting until sacrifice at day 7.

IVUS imaging

IVUS images of the rabbit aorta were acquired with a 40 MHz clinical catheter by automated 0.5mm/s pull back (iLab2, Polaris2 software imaging system, Boston Scientific, Marlborough, Massachusetts). The first IVUS pullback measured the artery size manually before balloon injury. The second IVUS pullback allowed calculation of the stent expansion ratio,

defined as the stent diameter at the stent middle divided by the distal reference diameter. IVUS datasets were analyzed by manual segmentation (OsiriX, Geneva, Switzerland).

Intravascular near-infrared fluorescence optical coherence tomography (NIRF-OCT) fibrin molecular-structural imaging

The intravascular NIRF-OCT imaging system and catheter have been described previously. Briefly, the catheter device contains a double clad fiber housing a single mode core that transmits 1310nm wavelength OCT light and a multimode inner cladding that transmits 750nm NIRF excitation light and receives emitted fluorescence light via the cladding from 765-855nm. The NIRF-OCT imaging system acquires co-registered NIRF and OCT data at speeds up to 25 frames per second and a pullback velocity of up to 20 mm/s. During NIRF-OCT imaging, blood clearance was performed by inflating an 0.035" 6.0mm diameter over-the-wire balloon (Armada 35, Abbott Vascular) in the proximal abdominal aorta via the carotid artery 5Fr sheath, and then flushing with a saline-contrast mixture was flushed during balloon inflation.

On day 7 after stent implantation, to assess in vivo fibrin-specific deposition on stent struts, rabbits underwent NIRF-OCT imaging with the fibrin-targeted NIRF molecular imaging agent FTP11-CyAm7[10]. Two hours after intravenous injection of 50 nmol/kg FTP11-CyAm7, rabbits were anesthetized and a 4Fr sheath was inserted into the left iliac artery and a 5Fr sheath into the right carotid artery. Next, NIRF-OCT pullback imaging was performed under saline-contrast flush was performed via the iliac artery, followed by sacrifice. The stented vessels were carefully resected and rinsed with saline followed by ex vivo imaging and histological analysis.

NIRF-OCT imaging analysis of stent coverage and fibrin-specific deposition

For stent coverage assessment, axial OCT cross-sectional images were analyzed at 400 □m intervals. Stent struts were classified as covered if tissue was visible over the stent strut **(Supplementary Figure 2)**. If a stent strut was not covered, it was classified as uncovered[10].

For quantitative measurement of NIRF fibrin signal on stent struts, NIR fluorescence data were obtained as previously described[10]. The NIRF signal was quantified using a distance compensation algorithm that corrects the NIRF signal intensity according to the distance between the intravascular imaging catheter and the vessel wall defined by the OCT image. The average NIRF fibrin signal intensity was measured at 400 um intervals across the stent. The background NIRF signal was averaged from two flanking non-stented segments at 2 mm proximal to the 3.5mm BP-SES and 2mm distal to the distal edge of the 3.0mm BP-SES. Target-to-background ratios (TBR) were calculated by dividing the target signal by the background signal intensity (Fig 1B). In vivo axial OCT images were co-registered to ex vivo axial fluorescence microscopy images along the longitudinal axis of the stent based on the stent edges as fiducials. Cross-

sectional NIRF-OCT images at 400 □m intervals were co-registered to histological images based on the distance from the stent edges. Angular co-registration was performed visually if fiducials such as side branches were absent.

Ex vivo fluorescence imaging

For ex vivo stent fibrin deposition imaging, a subset of resected stented vessels was cut longitudinally. The opened vessels with intact stents were imaged using an upright epifluorescence microscope (Nikon Eclipse 90i, Japan). The NIR channel (excitation/emission; 710/810nm) was used for FTP11-CyAm7 NIRF signal detection of fibrin deposition on stent struts[10].

Histopathology

For histopathological analysis, resected vessels were fixed with formalin and shipped to the German Heart Center (Munich, Germany). The explants encompassing the stented section of the artery and a 5-7mm non-stented arterial segment within the proximal and distal ends of the stents were processed in a graded series of alcohols and xylenes for embedding in methyl methacrylate and allowed to polymerize. Following complete polymerization, cross sectional tissue blocks were sawed using a precision diamond saw (Isomet 100, Buehler, Illinois). Tissue blocks were then mounted onto charged histology slides and consecutively cut at 10 microns using a laser microtome (Tissue surgeon, LLS Rowiak ROWIAK Laser Lab Solutions, Germany), polished and stained with H&E and Carstair's stain.

Pooled analysis of individual patient data from the BIOSCIENCE and BIOSTEMI trials

We performed an individual patient data pooled analysis from PCI patients enrolled in the BIOSCIENCE (*NCT02579031,* 2119 patients: 1063 BP-SES and 1056 durable-polymer everolimus-eluting stents, DP-EES) and BIOSTEMI (*NCT02579031,* 1300 patients: 649 BP-SES and 651 DP-EES) randomized clinical trials that compared clinical outcomes after BP-SES versus DP-EES implantation with respect to the primary endpoint of TLF at one-year of follow-up, and included a landmark analysis at 30 days. We included patients with chronic and acute coronary syndromes in the BIOSCIENCE trial and ST-elevation myocardial infarction (STEMI) patients enrolled in the BIOSTEMI trial, who received a single BP-SES. This pooled cohort of patients was next stratified into those treated with a single 3.0 mm BP-SES (strut thickness 60 μm) vs. those treated with a single 3.5 mm BP-SES (strut thickness 80 μm). We excluded patients with multiple lesions treated with BP-SES, and those patients with single lesions treated with multiple BP-SES, to attribute TLF events to a single BP-SES.

Statistical analyses

For preclinical studies, analyses were performed using Prism Software (v9.0, GraphPad Inc., La Jolla, CA). Data are shown as the mean ± SD. Differences between groups were examined by the two-tailed Student's t-test or two-way ANOVA, followed by Bonferroni's multiple comparison test. In all analysis, $p<0.05$ was considered statistically significant.

For clinical studies, P-values were obtained from chi-squared tests, t-tests, and Fisher's exact tests, as appropriate. We performed Mantel-Cox regressions using ordinary models as the BIOSCIENCE and BIOSTEMI randomized trials were intended to be combined using the same study centers and a historical prior based on the BIOSCIENCE data. Mantel-Cox logrank tests were used to calculate rate ratios (RR) and their associated 95% confidence intervals (CI) and p-values. We used time to first event for TLF endpoint and reported numbers of patients and Kaplan-Meier estimates of cumulative incidence. A p-value of <0.05 was considered statistically significant. Analyses were performed with Stata 17.0 (*StataCorp. 2023. Stata Statistical Software: Release 17.0. College Station, TX: StataCorp LLC*). The results are presented as counts with percentages for categorical variables, and as means ± standard deviations for continuous variables.

Supplementary Table 1. Medication at discharge, 30 days and 1 year of follow-up.

	BP-SES 3.0mm (60 □m)	**BP-SES 3.5mm (80 □m)**	**p-value**
	N = 282	**N = 222**	
At discharge			
Aspirin	276 (98.9%)	220 (99.5%)	0.634
Clopidogrel	83 (29.7%)	62 (28.1%)	0.693
Prasugrel	92 (33.0%)	79 (35.7%)	0.569
Ticagrelor	105 (37.6%)	77 (34.8%)	0.575
Any DAPT	276 (98.9%)	217 (98.2%)	0.705
VKA	14 (5.0%)	11 (5.0%)	1.000
Non-VKA anticoagulant	7 (2.5%)	3 (1.4%)	0.524
Statin	263 (94.3%)	215 (97.3%)	0.126
ACE inhibitor	179 (64.2%)	153 (69.2%)	0.253
β-blocker	208 (74.6%)	175 (79.2%)	0.243
At 30-day follow-up			
Aspirin	265 (98.1%)	215 (99.1%)	0.469
Clopidogrel	84 (31.1%)	66 (30.4%)	0.921
Prasugrel	88 (32.6%)	78 (35.9%)	0.443
Ticagrelor	96 (35.6%)	70 (32.4%)	0.501
Any DAPT	263 (97.4%)	211 (97.2%)	1.000
VKA	16 (5.9%)	15 (6.9%)	0.711
Non-VKA anticoagulant	7 (2.6%)	2 (0.9%)	0.310
Statin	255 (94.4%)	209 (96.3%)	0.394
ACE inhibitor	165 (61.1%)	142 (65.4%)	0.346
β-blocker	204 (75.6%)	166 (76.5%)	0.832
At 1-year follow-up			
Aspirin	256 (97.7%)	196 (96.6%)	0.573
Clopidogrel	77 (29.4%)	51 (25.1%)	0.346
Prasugrel	80 (30.5%)	67 (33.0%)	0.615
Ticagrelor	76 (29.0%)	55 (27.1%)	0.678
Any DAPT	226 (86.3%)	169 (83.3%)	0.433
VKA	14 (5.3%)	9 (4.5%)	0.830
Non-VKA anticoagulant	5 (1.9%)	3 (1.5%)	1.000

Statin	228 (87.4%)	181 (89.6%)	0.470
ACE inhibitor	137 (52.5%)	102 (50.5%)	0.708
β-blocker	182 (69.7%)	139 (68.8%)	0.840

Data are expressed as sample sizes (n) with counts (%). ACE, angiotensin converting enzyme; DAPT, dual antiplatelet therapy, VKA, vitamin K antagonist.

Supplementary Table 2. Clinical outcomes of BIOSTEMI only at 30 days and 1 year of follow-up.

	BP-SES 3.0mm (60 □m)	BP-SES 3.5mm (80 □m)	Rate ratio [95% CI]	p-value
	N = 98	N = 102		
At 30 days				
Death	5 (5.2)	0 (0.0)	13.53 (0.77-236.99)	0.013
Cardiac death	5 (5.2)	0 (0.0)	13.53 (0.77-236.99)	0.013
Myocardial infarction	1 (1.0)	0 (0.0)	1.73 (0.23-12.85)	0.616
Myocardial infarction Q-wave	1 (1.0)	0 (0.0)	1.73 (0.23-12.85)	0.616
Myocardial infarction non Q-wave	0 (0.0)	0 (0.0)	. (.-.)	.
TV Myocardial infarction	1 (1.0)	0 (0.0)	5.20 (0.25-106.95)	0.239
TV Myocardial infarction Q-wave	1 (1.0)	0 (0.0)	5.20 (0.25-106.95)	0.239
TV Myocardial infarction non Q-wave	0 (0.0)	0 (0.0)	. (.-.)	.
Cardiac death or MI (any)	6 (6.2)	0 (0.0)	5.90 (1.06-32.74)	0.017
Revascularisation (any)	2 (2.1)	0 (0.0)	2.43 (0.37-16.13)	0.361
Revascularisation (PCI)	2 (2.1)	0 (0.0)	2.43 (0.37-16.13)	0.361
Revascularisation (CABG)	0 (0.0)	0 (0.0)	. (.-.)	.
Revascularisation (TLR any)	1 (1.0)	0 (0.0)	5.20 (0.25-106.95)	0.239
Revascularisation (TLR clinically indicated)	1 (1.0)	0 (0.0)	5.20 (0.25-106.95)	0.239
Revascularisation (TVR clinically indicated)	1 (1.0)	0 (0.0)	5.20 (0.25-106.95)	0.239
Revascularisation (TVR any)	1 (1.0)	0 (0.0)	5.20 (0.25-106.95)	0.239

Cerebrovascular event (any)	0 (0.0)	0 (0.0)	. (.-.)	.
TIA	0 (0.0)	0 (0.0)	. (.-.)	.
Stroke (any)	0 (0.0)	0 (0.0)	. (.-.)	.
Stroke (ischemic)	0 (0.0)	0 (0.0)	. (.-.)	.
Target Lesion Failure (Cardiac death, TV-MI, TLR clinically indicated and TVR CA	6 (6.2)	0 (0.0)	17.69 (1.03-302.39)	0.003
Target Vessel Failure (Cardiac death, any Reinfarction, any TVR)	6 (6.2)	0 (0.0)	17.69 (1.03-302.39)	0.003
Death, MI or Revascularisation (any)	7 (7.3)	0 (0.0)	6.59 (1.20-36.06)	0.009
Stent thrombosis (definite)	1 (1.0)	0 (0.0)	5.20 (0.25-106.95)	0.239
Stent thrombosis (definite/probable)	4 (4.2)	0 (0.0)	11.45 (0.64-204.35)	0.027
At 365 days				
Death	6 (6.3)	0 (0.0)	13.53 (0.77-236.99)	0.013
Cardiac death	6 (6.3)	0 (0.0)	13.53 (0.77-236.99)	0.013
Myocardial infarction	2 (2.2)	1 (1.1)	2.19 (0.19-24.82)	0.515
Myocardial infarction Q-wave	2 (2.2)	1 (1.1)	2.19 (0.19-24.82)	0.515
Myocardial infarction non Q-wave	0 (0.0)	0 (0.0)	. (.-.)	.
TV Myocardial infarction	2 (2.2)	0 (0.0)	5.20 (0.25-106.95)	0.239
TV Myocardial infarction Q-wave	2 (2.2)	0 (0.0)	5.20 (0.25-106.95)	0.239
TV Myocardial infarction non Q-wave	0 (0.0)	0 (0.0)	. (.-.)	.

Cardiac death or MI (any)	8 (8.4)	1 (1.1)	8.78 (1.08-71.75)	0.014
Revascularisation (any)	3 (3.2)	1 (1.1)	3.31 (0.33-32.84)	0.278
Revascularisation (PCI)	3 (3.2)	1 (1.1)	3.31 (0.33-32.84)	0.278
Revascularisation (CABG)	0 (0.0)	0 (0.0)	. (.-.)	.
Revascularisation (TLR any)	2 (2.2)	0 (0.0)	5.20 (0.25-106.95)	0.239
Revascularisation (TLR clinically indicated)	2 (2.2)	0 (0.0)	5.20 (0.25-106.95)	0.239
Revascularisation (TVR clinically indicated)	2 (2.2)	0 (0.0)	5.20 (0.25-106.95)	0.239
Revascularisation (TVR any)	2 (2.2)	0 (0.0)	5.20 (0.25-106.95)	0.239
Cerebrovascular event (any)	0 (0.0)	1 (1.0)	0.35 (0.01-8.49)	1.000
TIA	0 (0.0)	0 (0.0)	. (.-.)	.
Stroke (any)	0 (0.0)	1 (1.0)	0.35 (0.01-8.49)	1.000
Stroke (ischemic)	0 (0.0)	1 (1.0)	0.35 (0.01-8.49)	1.000
Target Lesion Failure (Cardiac death, TV-MI, TLR clinically indicated and TVR CA	8 (8.4)	0 (0.0)	17.69 (1.03-302.39)	0.003
Target Vessel Failure (Cardiac death, any Reinfarction, any TVR)	8 (8.4)	0 (0.0)	17.69 (1.03-302.39)	0.003
Death, MI or Revascularisation (any)	9 (9.4)	1 (1.1)	9.97 (1.23-80.69)	0.008
Stent thrombosis (definite)	2 (2.2)	0 (0.0)	5.20 (0.25-106.95)	0.239
Stent thrombosis (definite/probable)	5 (5.3)	0 (0.0)	11.45 (0.64-204.35)	0.027
Depicted are nr of first events (% cumulative incidence from Kaplan-Meier estimate).				
Rate ratios (95% confidence intervals) and logrank P-values are from Mantel-Cox regressions.				

Number of first events (% cumulative incidence) from Kaplan-Meier estimate. Rate ratios, 95% confidence intervals (CI). MI, myocardial infarction; TLR, target lesion revascularization; TVR, target vessel revascularization; TIA, transient ischemic attack.

Supplementary Table 3. Clinical outcomes of BIOSCIENCE only at 30 days and 1 year of follow-up.

	BP-SES 3.0mm (60 mm)	BP-SES 3.5mm (80 mm)	Rate ratio [95% CI]	p-value
	N = 184	N = 120		
At 30 days				
Death	0 (0.0)	2 (1.7)	0.27 (0.08-0.92)	0.028
Cardiac death	0 (0.0)	1 (0.8)	0.22 (0.04-1.38)	0.081
Myocardial infarction	0 (0.0)	3 (2.5)	0.13 (0.02-0.74)	0.007
Myocardial infarction Q-wave	0 (0.0)	2 (1.7)	0.09 (0.00-1.73)	0.061
Myocardial infarction non Q-wave	0 (0.0)	1 (0.8)	0.22 (0.04-1.38)	0.081
TV Myocardial infarction	0 (0.0)	3 (2.5)	0.06 (0.00-1.08)	0.009
TV Myocardial infarction Q-wave	0 (0.0)	2 (1.7)	0.09 (0.00-1.73)	0.061
TV Myocardial infarction non Q-wave	0 (0.0)	1 (0.8)	0.13 (0.01-2.68)	0.155
Cardiac death or MI (any)	0 (0.0)	4 (3.3)	0.16 (0.04-0.62)	0.002
Revascularisation (any)	2 (1.1)	1 (0.8)	1.29 (0.12-14.37)	0.836
Revascularisation (PCI)	2 (1.1)	1 (0.8)	1.29 (0.12-14.37)	0.836
Revascularisation (CABG)	0 (0.0)	0 (0.0)	. (.-.)	.
Revascularisation (TLR any)	1 (0.5)	1 (0.8)	0.64 (0.04-10.45)	0.754
Revascularisation (TLR clinically indicated)	1 (0.5)	1 (0.8)	0.64 (0.04-10.45)	0.754
Revascularisation (TVR clinically indicated)	1 (0.5)	1 (0.8)	0.64 (0.04-10.45)	0.754
Revascularisation (TVR any)	1 (0.5)	1 (0.8)	0.64 (0.04-10.45)	0.754
Cerebrovascular event (any)	0 (0.0)	2 (1.7)	0.39 (0.05-2.91)	0.564
TIA	0 (0.0)	0 (0.0)	. (.-.)	.
Stroke (any)	0 (0.0)	2 (1.7)	0.39 (0.05-2.91)	0.564

Stroke (ischemic)	0 (0.0)	2 (1.7)	0.39 (0.05-2.91)	0.564
Target Lesion Failure (Cardiac death, TV-MI, TLR clinically indicated and TVR CA	1 (0.5)	4 (3.3)	0.16 (0.02-1.44)	0.060
Target Vessel Failure (Cardiac death, any Reinfarction, any TVR)	1 (0.5)	4 (3.3)	0.16 (0.02-1.44)	0.060
Death, MI or Revascularisation (any)	2 (1.1)	5 (4.2)	0.25 (0.05-1.32)	0.079
Stent thrombosis (definite)	0 (0.0)	1 (0.8)	0.09 (0.00-1.73)	0.061
Stent thrombosis (definite/probable)	0 (0.0)	4 (3.3)	0.05 (0.00-0.88)	0.004
At 365 days				
Death	3 (1.7)	8 (6.7)	0.24 (0.06-0.91)	0.023
Cardiac death	1 (0.6)	4 (3.4)	0.16 (0.02-1.44)	0.062
Myocardial infarction	1 (0.6)	7 (5.9)	0.09 (0.01-0.74)	0.005
Myocardial infarction Q-wave	0 (0.0)	3 (2.5)	0.09 (0.00-1.73)	0.061
Myocardial infarction non Q-wave	1 (0.6)	4 (3.4)	0.16 (0.02-1.44)	0.061
TV Myocardial infarction	0 (0.0)	5 (4.2)	0.06 (0.00-1.08)	0.009
TV Myocardial infarction Q-wave	0 (0.0)	3 (2.5)	0.09 (0.00-1.73)	0.061
TV Myocardial infarction non Q-wave	0 (0.0)	2 (1.7)	0.13 (0.01-2.68)	0.155
Cardiac death or MI (any)	2 (1.1)	10 (8.4)	0.13 (0.03-0.58)	0.002
Revascularisation (any)	10 (5.5)	6 (5.1)	1.09 (0.39-3.00)	0.871
Revascularisation (PCI)	10 (5.5)	6 (5.1)	1.09 (0.39-3.00)	0.871
Revascularisation (CABG)	1 (0.6)	0 (0.0)	1.96 (0.08-47.72)	1.000
Revascularisation (TLR any)	4 (2.2)	5 (4.3)	0.52 (0.14-1.93)	0.318
Revascularisation (TLR clinically indicated)	3 (1.7)	5 (4.3)	0.39 (0.09-1.62)	0.176

Revascularisation (TVR clinically indicated)	5 (2.8)	5 (4.3)	0.65 (0.19-2.24)	0.491
Revascularisation (TVR any)	6 (3.3)	5 (4.3)	0.78 (0.24-2.55)	0.676
Cerebrovascular event (any)	1 (0.6)	2 (1.7)	0.32 (0.03-3.59)	0.326
TIA	0 (0.0)	0 (0.0)	. (.-.)	.
Stroke (any)	1 (0.6)	2 (1.7)	0.32 (0.03-3.59)	0.326
Stroke (ischemic)	1 (0.6)	2 (1.7)	0.32 (0.03-3.59)	0.326
Target Lesion Failure (Cardiac death, TV-MI, TLR clinically indicated and TVR CA	4 (2.2)	10 (8.4)	0.25 (0.08-0.81)	0.012
Target Vessel Failure (Cardiac death, any Reinfarction, any TVR)	7 (3.9)	10 (8.4)	0.44 (0.17-1.17)	0.092
Death, MI or Revascularisation (any)	13 (7.2)	15 (12.5)	0.55 (0.26-1.16)	0.112
Stent thrombosis (definite)	0 (0.0)	3 (2.5)	0.09 (0.00-1.73)	0.061
Stent thrombosis (definite/probable)	0 (0.0)	6 (5.0)	0.05 (0.00-0.88)	0.004
Depicted are nr of first events (% cumulative incidence from Kaplan-Meier estimate).				
Rate ratios (95% confidence intervals) and logrank P-values are from Mantel-Cox regressions.				

Number of first events (% cumulative incidence) from Kaplan-Meier estimate. Rate ratios, 95% confidence intervals (CI). MI, myocardial infarction; TLR, target lesion revascularization; TVR, target vessel revascularization; TIA, transient ischemic attack.

Supplementary Table 4. Clinical outcomes at 1 year in patients that did not present with in-stent restenosis.

	BP-SES			
	Single stent 3.0 mm	**Single stent 3.5 mm**	**Rate ratio [95% CI]**	**Log rank p-value**
Number of patients	N = 263	N = 206		
Target lesion failure*	12 (4.6)	6 (3.0)	1.57 (0.59-4.18)	0.367
All-cause death	9 (3.5)	5 (2.5)	1.42 (0.47-4.24)	0.529
Cardiac death	7 (2.7)	2 (1.0)	2.75 (0.57-13.27)	0.188
Myocardial infarction	3 (1.2)	7 (3.5)	0.33 (0.09-1.29)	0.095
Myocardial infarction (Q-wave)	2 (0.8)	3 (1.5)	0.52 (0.09-3.14)	0.469
Myocardial infarction (non Q-wave)	1 (0.4)	4 (2.0)	0.20 (0.02-1.75)	0.104
Target vessel myocardial infarction	2 (0.8)	4 (2.0)	0.39 (0.07-2.14)	0.260
Target vessel myocardial infarction (Q-wave)	2 (0.8)	2 (1.0)	0.78 (0.11-5.60)	0.808
Target vessel myocardial (non Q-wave)	0 (0.0)	2 (1.0)	0.16 (0.01-3.31)	0.192
Cardiac death, or myocardial infarction	10 (3.9)	9 (4.5)	0.86 (0.35-2.13)	0.750
Any revascularization	10 (4.0)	4 (2.0)	2.00 (0.63-6.37)	0.234
Revascularization (PCI)	10 (4.0)	4 (2.0)	2.00 (0.63-6.37)	0.234
Revascularization (CABG)	1 (0.4)	0 (0.0)	2.35 (0.10-57.39)	1.000

Any target lesion revascularization	5 (2.0)	2 (1.0)	1.98 (0.38-10.21)	0.406
Clinically indicated target lesion revascularization	5 (2.0)	2 (1.0)	1.98 (0.38-10.21)	0.406
Clinically indicated target vessel revascularization	6 (2.4)	2 (1.0)	2.38 (0.48-11.80)	0.274
Any target vessel revascularization	6 (2.4)	2 (1.0)	2.38 (0.48-11.80)	0.274
Any cerebrovascular event	1 (0.4)	2 (1.0)	0.39 (0.03-4.37)	0.429
Transient ischemic attack	0 (0.0)	0 (0.0)	-	-
Any stroke	1 (0.4)	2 (1.0)	0.39 (0.03-4.37)	0.429
Ischemic stroke	1 (0.4)	2 (1.0)	0.39 (0.03-4.37)	0.429
Target vessel failure[#]	13 (5.0)	6 (3.0)	1.70 (0.64-4.47)	0.278
Death, myocardial infarction, or any revascularization	19 (7.4)	11 (5.5)	1.36 (0.65-2.87)	0.414
Definite stent thrombosis	2 (0.8)	2 (1.0)	0.79 (0.11-5.61)	0.810
Definite/probable stent thrombosis	5 (1.9)	4 (2.0)	0.97 (0.26-3.64)	0.968

Depicted are number of first events (% cumulative incidence from Kaplan-Meier estimate). Rate ratios (95% confidence intervals) and log rank P-values are from Mantel-Cox regressions. Interaction p-value from heterogeneity test (approximate chi-square test). BP-SES, biodegradable polymer sirolimus-eluting stents; CABG, coronary artery bypass grafting; CI, confidence interval; DP-EES, durable polymer everolimus-eluting stents; PCI, percutaneous coronary intervention. *composite of cardiac death, target vessel myocardial infarction, or clinically indicated target lesion revascularization. [#] composite of cardiac death, target vessel myocardial infarction, or clinically indicated target vessel revascularization.

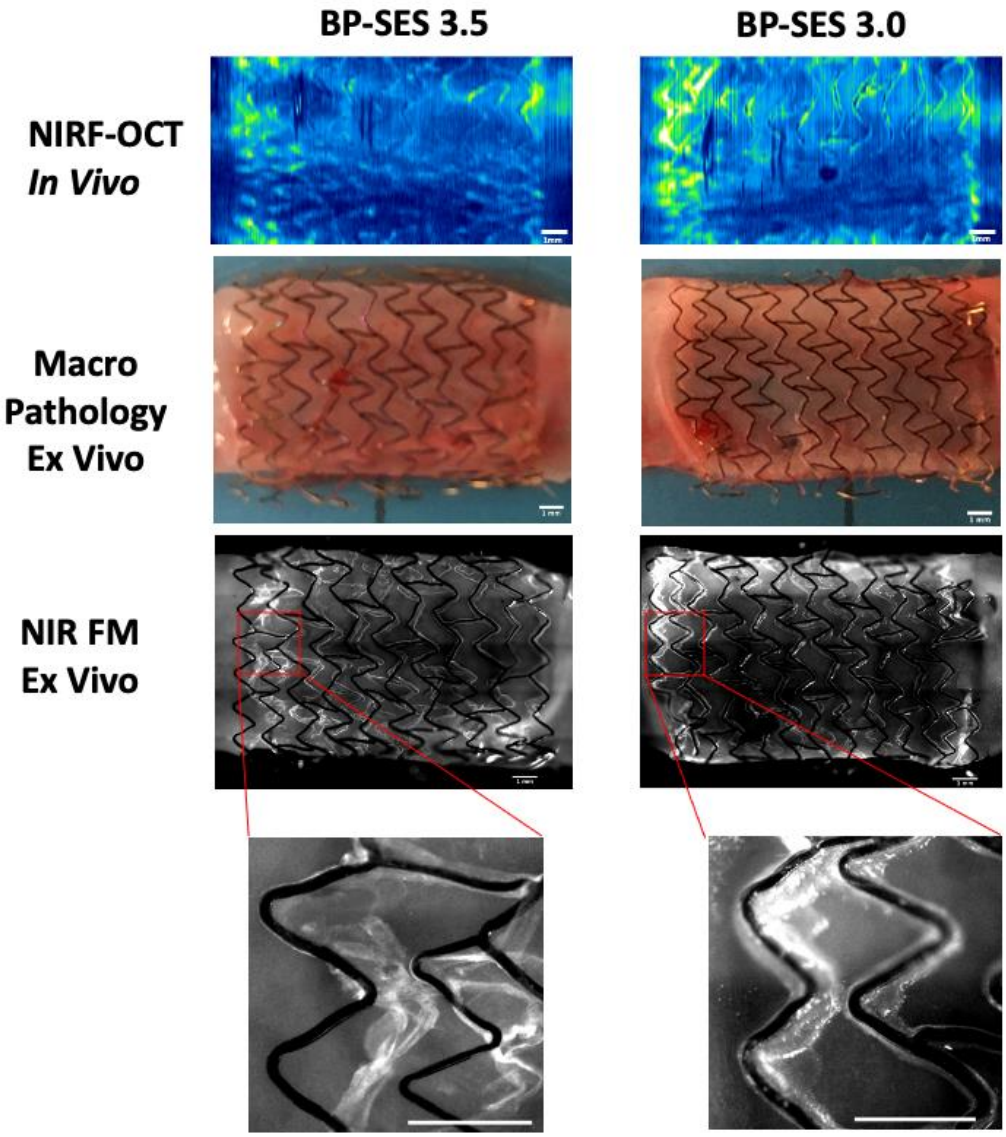

Supplementary Figure 1. *Ex vivo* NIRF molecular imaging of fibrin deposition on BP-SES stents.

Rabbits (n=8) underwent implantation of non-overlapping 3.5mm and 3.0mm BP-SES into the infrarenal aorta, followed by FTP11-CyAm7 intravenous injection at day 7, NIRF-OCT, and then sacrifice. Representative images of in vivo distance-corrected NIRF 2D fibrin maps, the endoluminal surface on fluorescence microscopy after longitudinally opening stents, FM, fluorescence microscopy. Scale bar, 1mm.

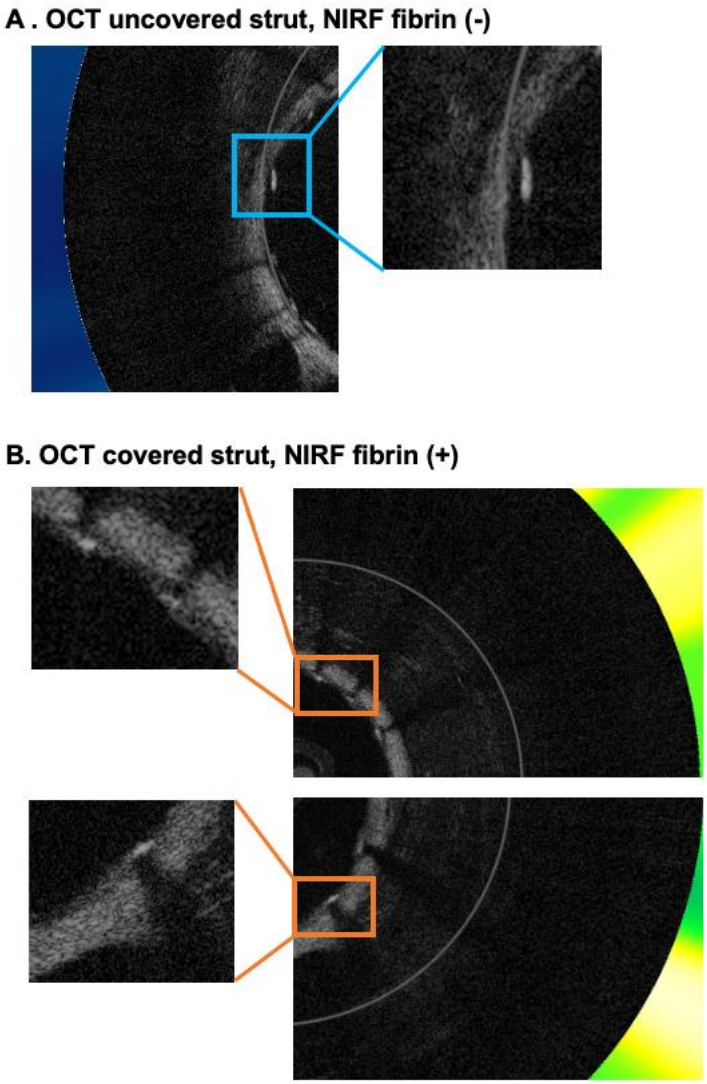

Supplementary Figure 2. NIRF-OCT fibrin assessment of uncovered and covered stent struts. **A**. Representative NIRF-OCT axial images of uncovered stent struts. **B**. Representative NIRF-OCT axial images of covered stent struts, showing NIRF-positive areas indicating fibrin deposition on stent struts.